PNNL-13111

Predicted Performance of Neutron Spectrometers Using Scintillating Fibers

R. A. Craig
M. Bliss

February 2000

Prepared for the U.S. Department of Energy
Under Contract DE-AC06-76RLO 1830

PACIFIC NORTHWEST NATIONAL LABORATORY
operated by
BATTELLE MEMORIAL INSTITUTE
for the
UNITED STATES DEPARTMENT OF ENERGY
under Contract DE-AC06-76RLO 1830

Printed in the United States of America

**Available to DOE and DOE contractors from the
Office of Scientific and Technical Information, P.O. Box 62, Oak Ridge, TN 37831;
prices available from (615) 576-8401.**

**Available to the public from the National Technical Information Service,
U.S. Department of Commerce, 5285 Port Royal Rd., Springfield, VA 22161**

PNNL-13111

Predicted Performance of Neutron Spectrometers Using Scintillating Fibers

R. A. Craig
M. Bliss

February 2000

Prepared for the U.S. Department of Energy
Under Contract DE-AC06-76RLO 1830

Pacific Northwest National Laboratory
Richland, Washington 99352

Summary

One class of neutron spectrometers is devices that provide a measure of the neutron spectrum by using moderating and absorbing materials together with thermal-neutron detectors. Pacific Northwest National Laboratory has developed scintillating fibers that are sensitive to thermal neutrons. Because these fibers are thin, they present an enabling technology for several applications, including highly efficient neutron spectroscopy. The underlying concept is to arrange the fibers in an array of layers separated by materials whose characteristics have been chosen to optimize the instrument function for the application. Monte Carlo experiments have been performed to characterize the conceptual design and to determine the value of the concept as a tool for research and other applications.

Acknowledgements

The authors want to thank A. J. Peurrung, B. D. Geelhood, and G. Dudder for many helpful and constructive discussions. Pacific Northwest National Laboratory is operated for the U.S. Department of Energy by Battelle under Contract DE-AC06-76RLO 1830.

Contents

Figures

1.0 Introduction

A variety of needs exists for knowing the energy spectral content of a neutron flux. Among these needs are arms-control and national-security applications, which arise because different neutron sources produce different neutron energy spectra. This work is primarily directed at these applications.

The concept described herein is a spectrometer in the same sense as a Bonner sphere. The instrument response reflects a statistical average of the energy spectrum. The Bonner sphere is an early rendition of this class. In this, a neutron detector is placed at the center of a moderating (and absorbing) sphere (of varying thickness and composition). Spectral unfolding is required, and the resolution and efficiency are, typically, poor, although the potential bandwidth is very large. A recent variation on the Bonner-sphere approach uses ^{3}He gas proportional counters with resistive wires to locate the position of the event (Toyokawa et al 1996).

The spectrometer concept investigated here has the potential for better resolution and much improved neutron efficiency compared to Bonner spheres and similar devices. These improvements are possible because of the development of neutron-sensitive, scintillating-glass fibers. These fibers can be precisely located in space, which allows a corresponding precision in energy resolution. Also, they can be fabricated into arrays that intercept a large fraction of incident thermal neutrons, providing the improvement in neutron economy.

An improvement such as this has numerous potential applications within the national security mission and in other areas. For the purposes of this analysis, which is primarily intended to provide design guidance, the focus is on the ability to distinguish between different neutron spectra. It is important to recognize that the universe of applications extends well beyond this.

It is also important to note that, in an actual application, the spectrometer will be exposed to neutrons directly from the source plus others that are best described as environmental, i.e., those that have originated from the source (or other sources) and have reflected off the environment. This analysis considers only the response of the spectrometer to the primary neutron source. A limited analysis of the effect of environmental interactions is included as Appendix B.

2.0 Scintillating Fibers

Cerium-activated, lithium-silicate glass scintillates in the presence of a thermal neutron flux. At Pacific Northwest National Laboratory (PNNL), these glasses are drawn into scintillating waveguides using a hot-downdraw tower. The use of a hot-downdraw system avoids crystallization of the lithium-rich glass. The glass fiber is clad with a thermal-curing silicone rubber that serves as both an optical cladding and a physical buffer. The cladding polymer was selected to give the waveguides a large numerical aperture. The numerical aperture determines the fraction of photons that will be confined inside the fiber. For these fibers, the captured fraction is approximately 0.033 towards each end.

Applications for the fibers are based on detecting scintillation photons induced in the glass by a $^{6}Li(n,\alpha)^{3}H$ reaction. This reaction is exothermic, releasing approximately 4.7 MeV, of which the majority is carried away by the triton. The triton and alpha particle each interact with the glass matrix to produce an ionization trail. This ionization transfers energy by exciting Ce^{3+} ions, which scintillate with the emission of photons of wavelength ca. 400 nm.

The scintillating glass is sensitive to Compton electrons and photoelectrons produced by gamma rays as well as neutrons. Electrons, however, produce much smaller pulses than neutrons. Because the range of Compton electrons is much greater than the 120-μm diameter of the fiber, the full electron energy is rarely deposited in a single fiber. A distinct neutron signature based on pulse amplitude makes it possible to use electronic logic circuitry to separate neutron-induced signals from other events. This report considers only the effects of neutrons. The gamma-ray response provides additional information about the character of the source. This information will be examined after the prototype spectrometer is built.

3.0 Specification of the Problem

The application for which this assessment was conducted is one of arms control or nonproliferation. It is desirable to be able to determine if the contents of a container are what they claim to be. Neutron spectroscopy offers one possibility for performing that determination. The specifications for the spectrometer system were predicated on the type of equipment that has traditionally been used for these activities and on practicality considerations:

- portable (i.e., no more than 20 kg for the detector)
- efficient enough to require a short counting time (i.e., approximately 5-min count for 6×10^4 n/sec source)
- simple to fabricate (i.e., no more than six fiber bilayers and no more than 60 km of fiber).

Within these limitations, two configurations were considered: a planar configuration and a cylindrical configuration. The purpose of considering two configurations is to explore and demonstrate the strength of the underlying concept and to determine which configuration is superior for this application.

The choice of configurations is predicated, in part at least, on prior work. A planar configuration is simple in concept and easy to fabricate, it is the obvious extension of previous scintillating fiber configurations (Seymour et al. 1988; Bliss et al. 1995; Bliss and Craig 1995), and it has been theoretically explored earlier (Bliss, Craig, and Sunberg 1997). The earlier scoping studies showed that the response of a fiber layer located about 5 cm from the front surface is relatively insensitive to the energy of the incident neutron. This means that the information content of the signal from layers in this region is smaller than that at other depths. The response of shallower layers distinguishes between low-energy neutrons; the response of deeper layers distinguishes between higher energy neutrons. For this reason, fiber layers were not distributed uniformly. As a practical matter, locating fiber layers closer than about 1-cm apart is problematic; so, for this analysis, the six fiber layers were located at depths of 2, 3, 5, 7, 8 and 9 cm, respectively.

The fiber and moderator layers form concentric cylinders in the second configuration, which is cylindrical. This configuration is somewhat more difficult to fabricate than the planar configuration. It provides improved efficiency because neutrons can reflect around the hollow center with multiple opportunities for detection; it will have a more complicated instrument-response function, but is known from previous work to be satisfactory (Hezeltine 1998). The configurations addressed are shown in Figures 3.1 and 3.2.

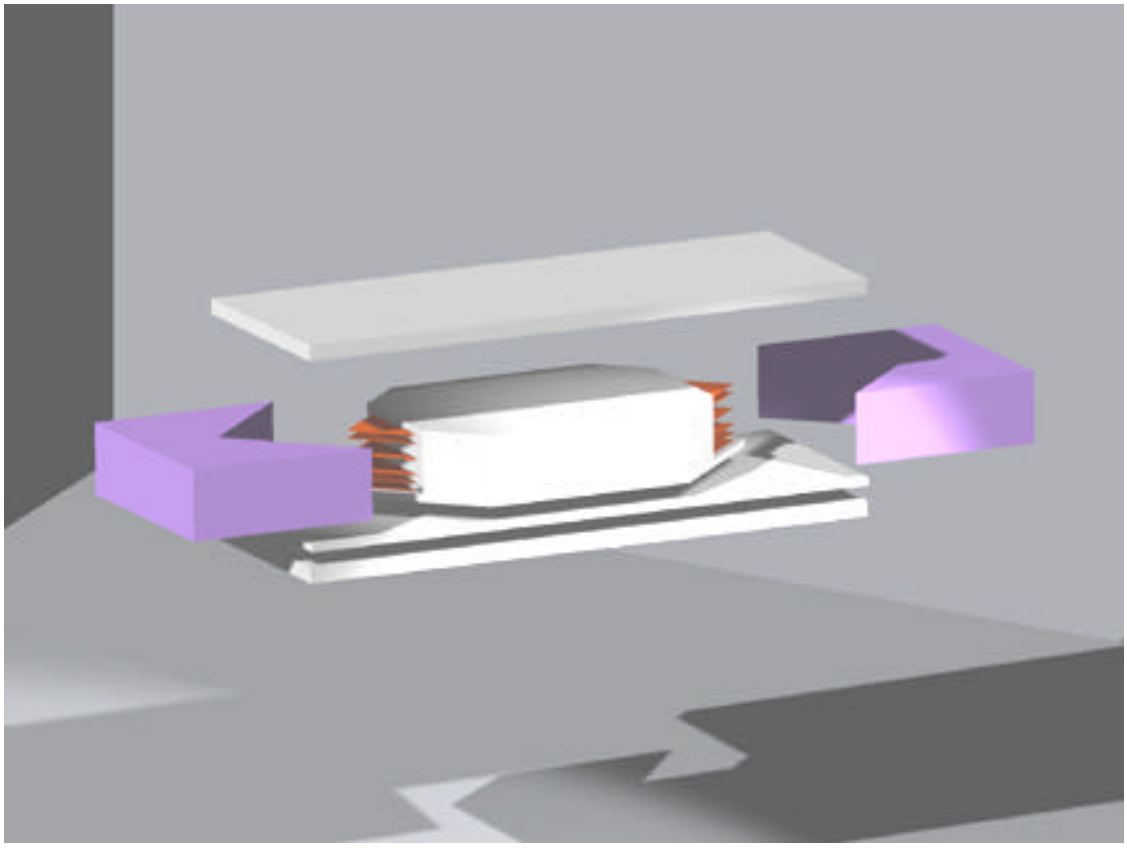

Figure 3.1. Exploded View of Planar Configuration for Neutron Spectrometer, as Modeled. Colored end pieces are polyethylene foam; white areas are UHMW polyethylene; 1-cm layers of UHMW are separate fiber bilayers; the unmarked volume is filled with Hi-Gell® protective polymer.

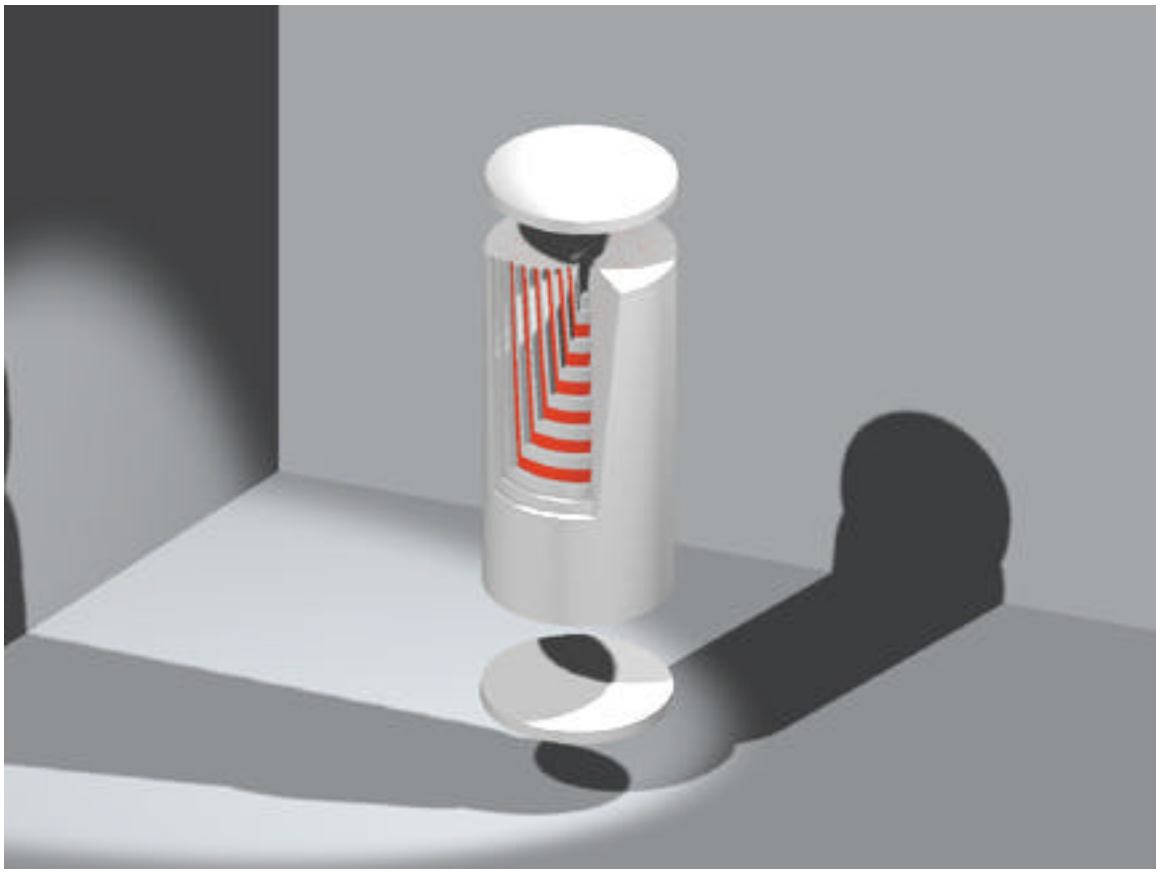

Figure 3.2. Exploded View of Cylindrical Configuration for Neutron Spectrometer, as Modeled. White cylinders and end caps are UHMW polyethylene. Colored areas are fiber bilayers.

Seven neutron spectra were chosen for preliminary analysis. This selection was chosen to provide a sampling of commonly available neutron sources and to test the performance of the technique. The source spectra are those for ^{252}Cf and ^{240}Pu spontaneous fission[1] and PuBe (Knoll 1989, p. 23), oxygen, and fluorine (α,n) reactions at 5 and 5.5 MeV (corresponding to ^{239}Pu and ^{241}Am α-particle sources respectively) (Matsunobu et al. 1992). These neutron spectra are shown in Figures 3.3 through 3.6. The Pu and Cf spontaneous spectra are quite similar, differing in the components with energy greater than 1 MeV; the PuBe (α,n) spectrum is very different from the Pu and Cf spectra and from the oxide and fluoride (α,n) spectra; the PuF and PuO sources are quite different, the PuF source more resembling the Pu and Cf spectra;[2] the fluorine (α,n) spectra for 5.0 and 5.5 MeV are quite similar, differing only in a slight shift of the peak and the magnitude of the low-energy peak.

[1] MCNP4a: Monte Carlo N-Particle Transport Code System, distributed by Radiation Shielding Information Center at Oak Ridge National Laboratory.

[2] Note that, if the plutonium from which the PuF and PuO spectra are derived contains ^{240}Pu, there will be spontaneous neutrons from fission of ^{240}Pu. The spectra in Figures 3.4 through 3.6 are only the (α,n) parts. For a typical, fresh, weapons-grade material, the (α,n) reactions contribute about 50% of the neutrons from PuO and about 98% of those from PuF.

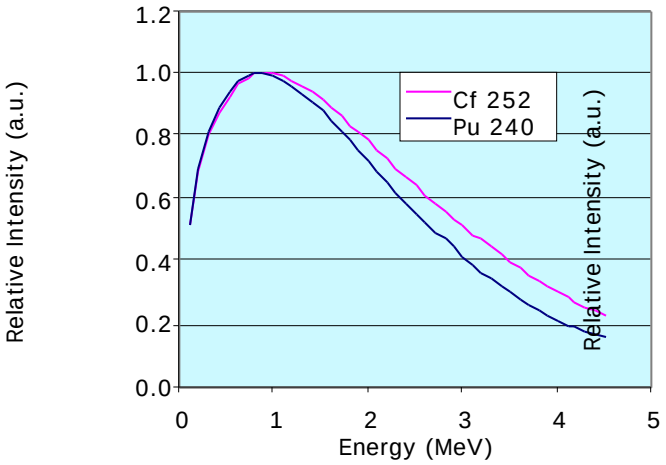

Figure 3.3. Neutron Spectra for Spontaneous Fission of ^{252}Cf and ^{240}Pu

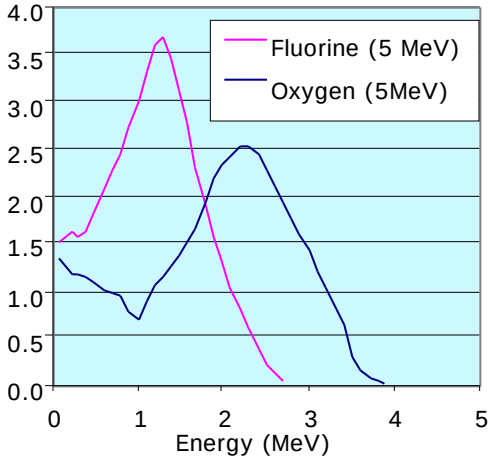

Figure 3.4. Oxide and Fluoride (α,n) Neutron Spectrum for Alpha-Particle Energies of 5 MeV, Corresponding to ^{239}Pu Oxide and Fluoride Sources

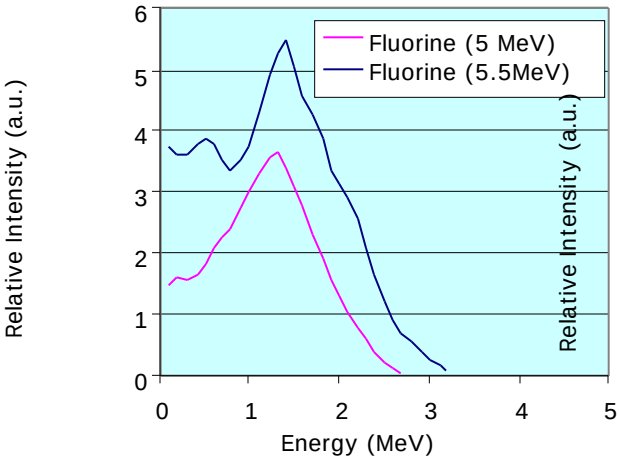

Figure 3.5. Fluorine (α,n) Neutron Spectrum for Alpha-Particle Energies of 5 and 5.5 MeV, Corresponding to ^{239}Pu and ^{241}Am Sources

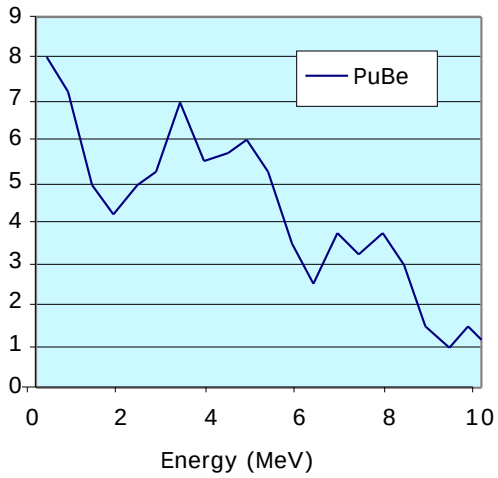

Figure 3.6. PuBe (α,n) Neutron Spectrum. Note difference in energy scale between this figure and other neutron spectra

4.0 Performance Metric

To evaluate the performance of the instrument design, for the specific application of distinguishing between neutron spectra, two steps are required. First, the response of the detector to each neutron spectrum is determined. Then, the two data sets are compared. This comparison, i.e., the performance, requires a suitable definition.

Definition of the Metric

In this case, the sets of data, i.e., the spectral measurements, to be compared are treated as points in an n-dimensional space. The measure of similarity of the two spectral measurements is taken to be the Euclidian distance between the points.

For application to the spectrometer, the data are the number of counts in each of the n layers for a given period of time or a given sum of the total number of counts in all layers. Each set of data from the six layers is a point in n-dimensional space. If x_i is the "correct" value of a point in n-space, as determined by a series of measurements, and y_i is the result of a measurement, then a single criterion, S, for the similarity of the measurement to the correct value is

$$S^2_{ac} = \Sigma (a_i - c_i)^2 \tag{4.1}$$

where the sum is over i and the c and a are appropriately scaled measures of x_i and y_i, respectively. Scaling may be necessary so that the information content of each dimension is treated equally. Small distances imply similarity; large distances imply dissimilarity.

This method is called the "mean-squared-distance" algorithm and is related to a Chi-squared-fit approach that was successfully applied in an ultrasonic signatures technique (Good et al. 1993). Because the data are uncorellated and statistically well-behaved, the variance is well-approximated by the square root of the mean, $\underline{n}_i$. Therefore, in the analysis of the distance between points weighted by the variance, the actual quantity evaluated is[1]

$$S^2_{ac} = \sum \frac{1}{2} \left[\frac{\left(n_i - \underline{n}_i\right)^2}{n_i} \right] \tag{4.2}$$

The importance of this choice of scaling is clarified when statistical noise is added to the problem. Assuming normal distributions for the counts in each layer,

$$P(n_1, n_2, \ldots n_6) \sim P(n_1) \bullet P(n_2) \ldots P(n_n)$$

$$\sim \left[\exp\left[-\frac{\left(n_1 - \underline{n}_1\right)^2}{2\sigma_1^{\,2}} \right] \right] \cdot \left[\exp\left[-\frac{\left(n_2 - \underline{n}_2\right)^2}{2\sigma_2^{\,2}} \right] \right] \ldots \left[\exp\left[-\frac{\left(n_6 - \underline{n}_n\right)^2}{2\sigma_n^{\,2}} \right] \right]$$

[1] The factor of 1/2 is chosen for convenience in statistical analysis.

$$\sim \{\exp[-(\xi_1^2)]\} \bullet \{\exp[-(\xi_2^2)]\} \ldots \{\exp[-(\xi_n^2)]\} \tag{4.3}$$

where $\xi_I = (n_i - \underline{n_i})/\sqrt{2}\sigma_I$ or

$$P(n_1, n_2, \ldots n_n) \sim \{\exp[-(\rho^2)]\} \tag{4.4}$$

where

$$(\rho^2) = \xi_1^2 + \xi_2^2 + \ldots + \xi_n^2 \tag{4.5}$$

is the "total mean-square distance" and is readily seen to be identical to S^2.

When the dimensionality, i.e., the number of fiber layers, is six, it is readily shown that the distribution for ρ is

$$P(\rho)d\rho = \rho^5\{\exp[-(\rho^2)]\}\ d\rho \tag{6}$$

This distribution is a toroidal shape in 6-space and peaks (the most probable value of ρ at a value of $\rho \sim 1.6$. (Figure 4.1). The arrows in Figure 4.1 show the values of ρ for which the probability of exceeding that value is 0.01, 0.001, and 0.0001, respectively.

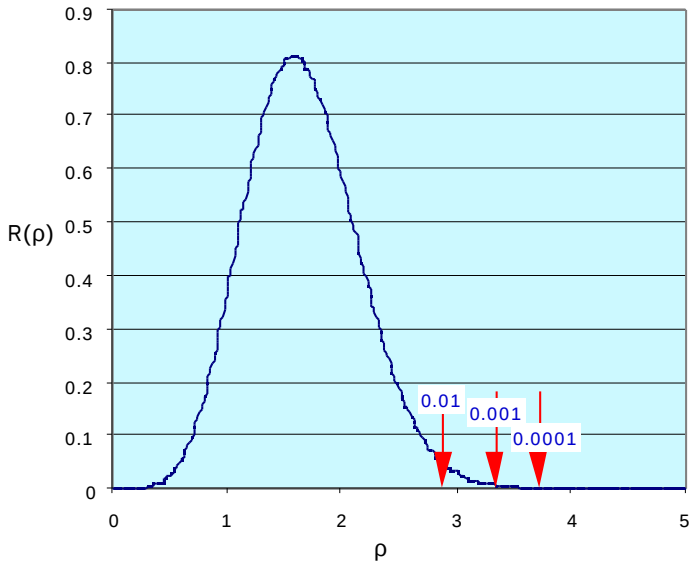

Figure 4.1. The Probability Density R(ρ) vs. ρ. The arrows show the values of ρ for which the probability of exceeding that value is 0.01, 0.001, and 0.0001, respectively.

This distribution is quite different from the usual Gaussian distribution (from which it is derived)[1] and is compared with a Gaussian distribution in Table 4.1. The factor of ρ^5 preceding the exponential significantly spreads out the distribution. Combining the information from the different layers can improve the confidence that a difference in signal between a measurement and a standard is real, but it also increases the number of ways that statistical fluctuations can add to produce an erroneous result. Physically, this means that the information gained by adding a layer must be very carefully weighed against the statistical noise introduced by adding an additional degree of freedom. This is briefly discussed in Appendix A.

Table 4.1. Value of _ for Which Value is Exceeded by Chance

Odds that value is exceeded by chance	Gaussian distribution	R(_) (dimensionality = 6)
1:1	0.48	1.6
$1:10^2$	1.8	2.9
$1:10^4$	2.3	2.7
$1: 10^6$	3.1	3.4
$1: 10^7$	3.5	3.7

4.1 Scenarios

The response of the spectrometers is calculated for two scenarios. In the first, the detector counts for a fixed period of time (the constant-time scenario) and the number of counts in each of the fiber layers in the spectrometer is calculated. In the second, the detector counts until a fixed number of total counts (that is, the sum of counts in the six layers) is collected (the constant-count scenario). In all cases, the source is taken to be emitting $6 \bullet 10^4$ neutrons per second, corresponding to the neutron emissions of approximately 1 kg of weapons-grade (WG) plutonium.

The constant-time scenario is representative of that which is incorporated into a typical experiment. It presupposes a representation that whatever is being presented for test is the item (either individual or type) for which the standard spectrum was measured. The constant-number-of-count scenario is more representative of one in which an unknown is to be identified.

[1] NB: ρ^2 is $(n\text{-}n)^2/2\sigma$, where σ is the variance. The factor of two, convenient for analysis, is also different from the conventional expression.

5.0 Evaluation of the Designs

For purposes of modeling, the source was located 1 m from the front surface of the detector. A total of $5 \cdot 10^7$ neutron histories was run for each analysis, giving a variance of approximately 1%. The neutron simulation code, MCNP4a, was run for a series of incident neutron energies[1]; the response of each fiber layer was calculated. (Figure 5.1. shows the response of the layers of the planar detector vs. energy.) Then the response, for each fiber layer, was fit to a polynomial in the logarithm of energy (Figure 5.2). From this polynomial fit, the layer-by-layer response is calculated for each neutron energy spectrum (Figures 3.3 through 3.6) and the scaled mean-square displacement metric was calculated for each pair of spectra.

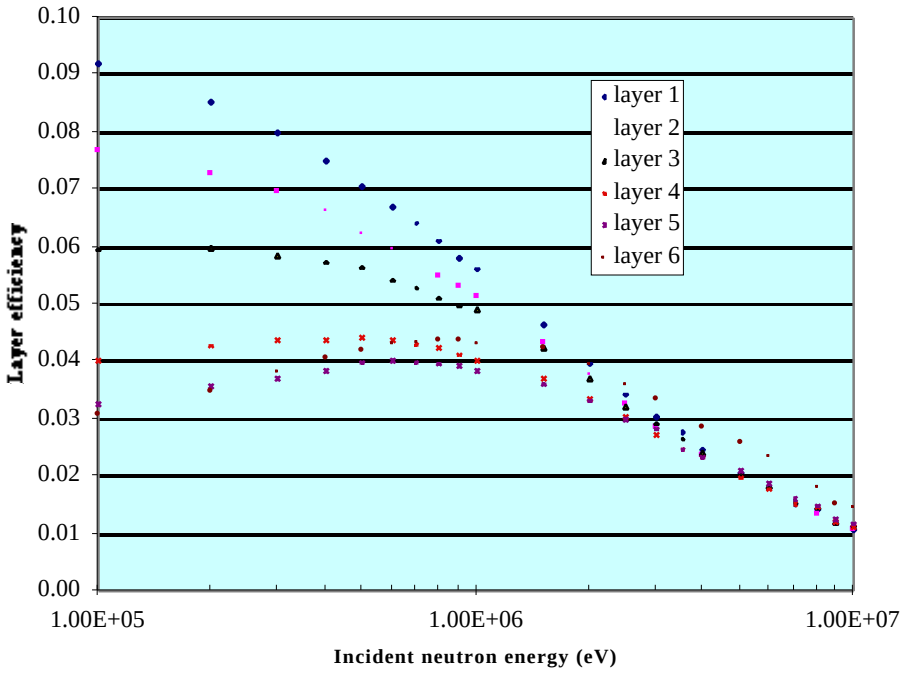

Figure 5.1. Layer-by-Layer Response of the Planar Spectrometer as a Function of Energy[2]

[1] 0.1 to 1.0 MeV by 0.1 MeV, 1.0 to 4.0 MeV by 0.5 MeV and 4.0 to 10.0 MeV by 1 MeV.

[2] This figure is comparable with Figure 15-2 of Knoll (pg. 517, op cit.) in which the energy dependence of a Bonner sphere is being discussed. Note that: 1) Figure 5.1 (here) covers the region from 10^{-1} to 10^{1} MeV and 2) for the fiber spectrometer, all layers can be read out simultaneously.

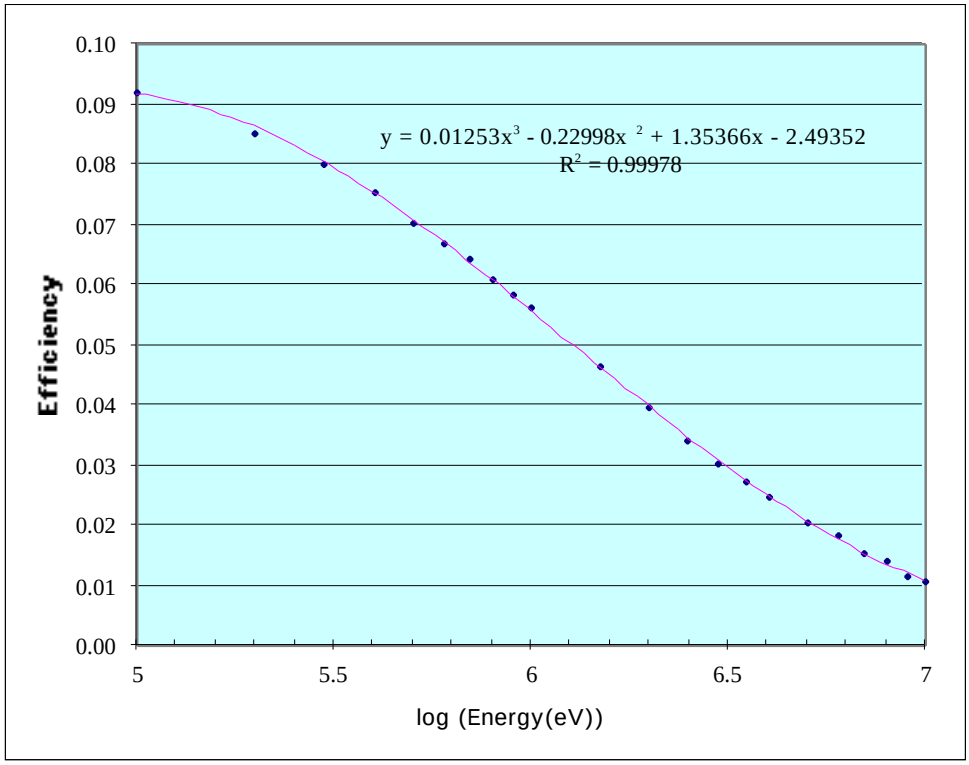

Figure 5.2. Third-Order Fit of the Response of the First Bilayer of the Planar Detector as a Function of Energy

6.0 Results

The modeling results are used to perform a relative evaluation of the two configurations for the design conditions. A sensitivity analysis, including the ability to separate various mixes of WG Pu and PuO; and a preliminary analysis of the information content of each layer, developed using these results, is provided in Appendix A.

6.1 Evaluation of Configurations

The values of ρ, corresponding to comparison of the calculated responses of the two configurations to the various neutron sources, is shown in Figure 6.1 and Figure 6.2. Figure 6.1 shows the comparison of the test spectrum with the standard spectrum for the scenario in which the counting is performed until $3.5 \bullet 10^4$ total events are scored in the detector. The diagonal boxes are identically zero because, for these, the test and standard spectra are identical. The red boxes represent comparisons for which the value of ρ is sufficiently small that there is greater than an equal probability of likes being mistaken for unlikes because of statistical variations. The yellow boxes represent comparisons for which the probability of randomly mistaking likes for unlikes is less than 1:2, but greater than a 1:10,000 probability status. The green boxes represent situations for which the probability of likes being randomly mistaken for unlikes is smaller than 1:10,000. White boxes represent the situations for which the spectra are identical.

The planar spectrometer is superior to the cylindrical version in distinguishing between likes and unlikes. Because the value of ρ scales as the square root of the number of counts recorded, calculation for a greater number of counts is straightforward. For instance, to address the situation in which $7 \bullet 10^4$ counts are recorded, each of the ρ values in Figure 6.1 would be multiplied by 1.41. For the planar configuration, the only effect that that change would have would be to move the comparison of the Cf fission spectrum with that of the Pu fission spectrum into the 1:10,000 category.

The predicted time for recording $3.5 \bullet 10^4$ counts is shown across the bottom of the matrices. It is seen that the times are slightly shorter for the cylindrical detector than for the planar; that is, the efficiency of the cylindrical detector is slightly greater than that of the planar configuration. This increase in efficiency occurs because there are no edges, out of which neutrons might be lost, for the cylindrical configuration.

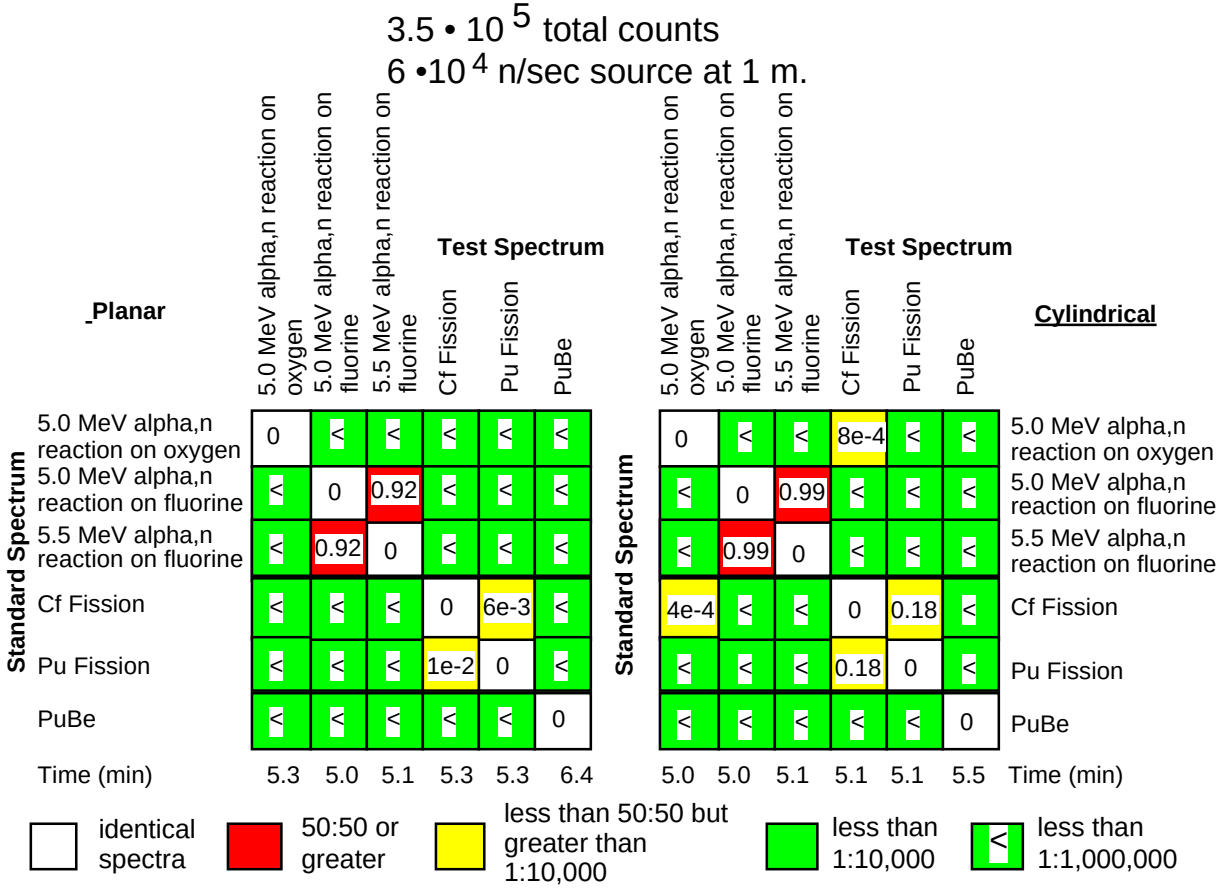

Figure 6.1a. Predicted Performance of Planar and Cylindrical Spectrometers for the Fixed-Count Scenario. The numbers in the box represent the probability of likes being mistaken for unlikes because of statistical variations. The symbol < indicates that the chance of a measurement producing the erroneous conclusion is less than 1 in 10^{-6}. The colors in the boxes provide a qualitative estimate of this probability.

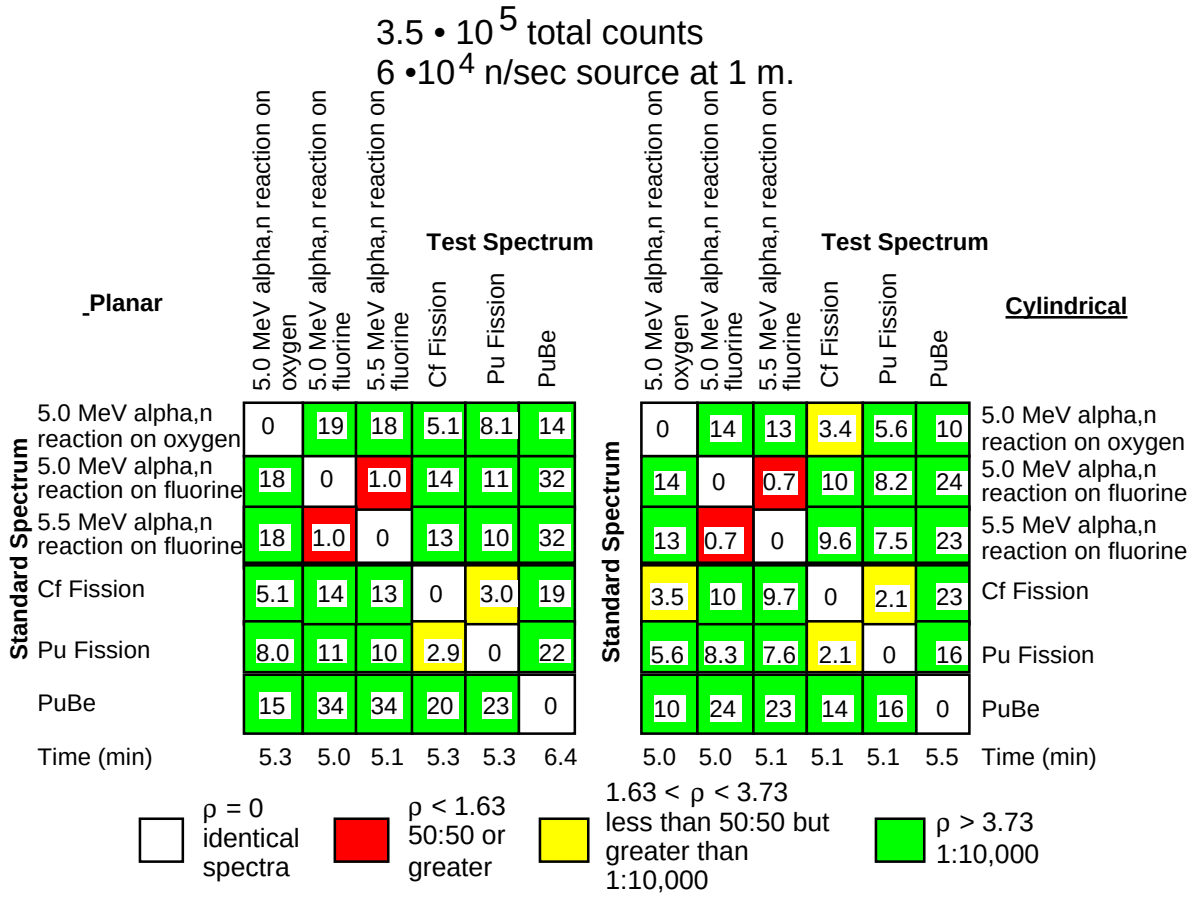

Figure 6.1b. Predicted Weighted Mean-Square Distance Performances of Planar and Cylindrical Spectrometers for the Fixed-Count Scenario. The weighted mean square distance for each situation is shown in the respective box. Values of $\rho = 0$ imply identical spectra; values less than 1.63 mean that the measurement is sufficiently similar to the standard that they have equal probability, or greater, of having been generated by the same spectrum; values of ρ greater than 3.73 mean that there is less than 1 chance in 10,000 that the measurement and standard were generated by the same spectrum..

Figure 6.2 shows the comparison of the test spectrum with the standard spectrum for the scenario in which the counting is performed for a fixed period of 5 min for a source of $6 \cdot 10^4$ neutrons per second, corresponding to approximately 1 kg of WG Pu[1]. The box marking has the same meaning as for Figure 6.1. Here, as in the constant total number of counts scenario, the planar configuration is generally superior to the cylindrical configuration.

The constant-count-time scenario is superior at distinguishing between likes and unlikes than the constant-count scenario, even when ρ is scaled to make the counting times more similar. This difference arises in the differences in total energy-integrated efficiencies (of the detector) for the different sources. The information content of the performance metric lies in two parts: 1) the detector total efficiency and 2) the differential efficiency of the fiber layers. For the constant-total-count scenario, the first of these is not used. Note that in order to improve the separation of the fluorine (α,n) spectra to better than 1% confidence in the constant-count-time scenario, it is only necessary to extend the count time to 5.5 min from 5 min.

[1] R. Brodzinski, Memorandum to Distribution, "Neutron Yields from Plutonium Oxide," March 18,1993.

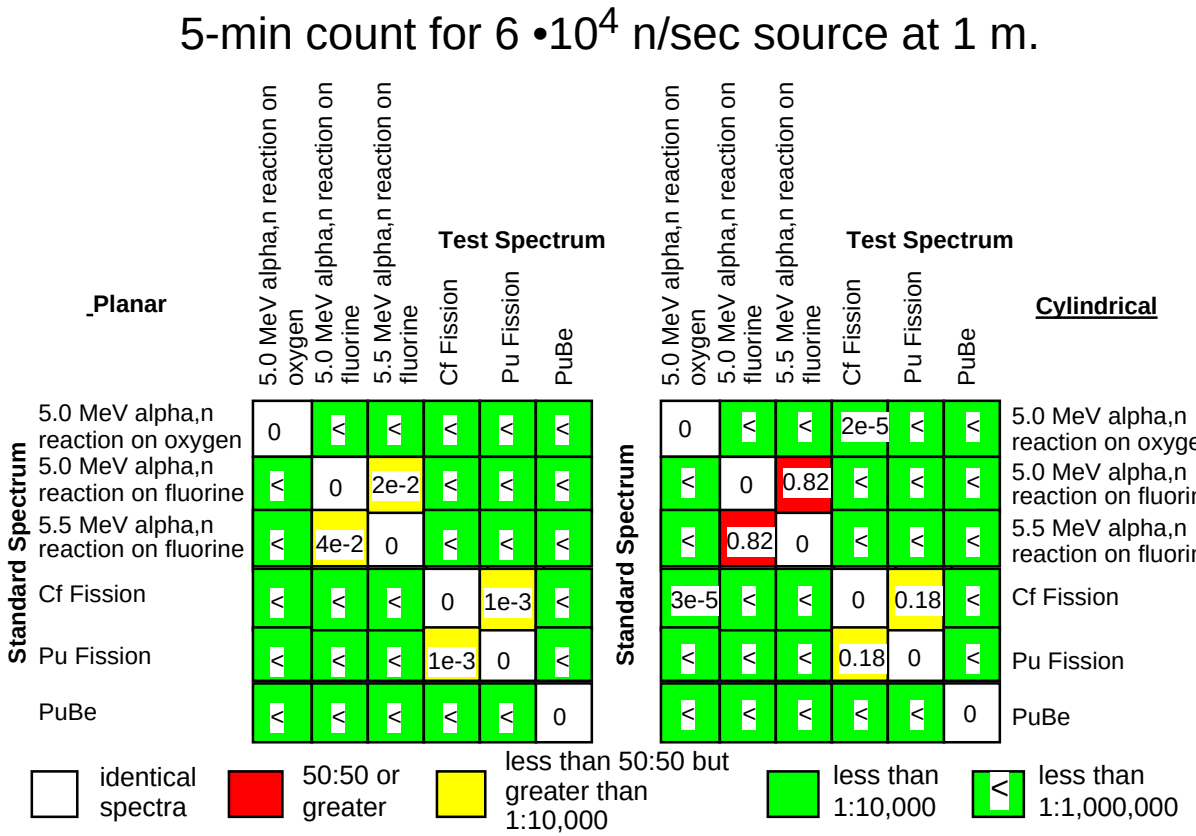

Figure 6.2a. Predicted Performance of Planar andCylindrical Spectrometers for the Fixed-Count Scenario. The numbers in the box represent the probability of likes being mistaken for unlikes because of statistical variations. The symbol < indicates that the chance of a measurement producing the erroneous conclusion is less than 1 in 10^{-6}. The colors in the boxes provide a qualitative estimate of this probability.

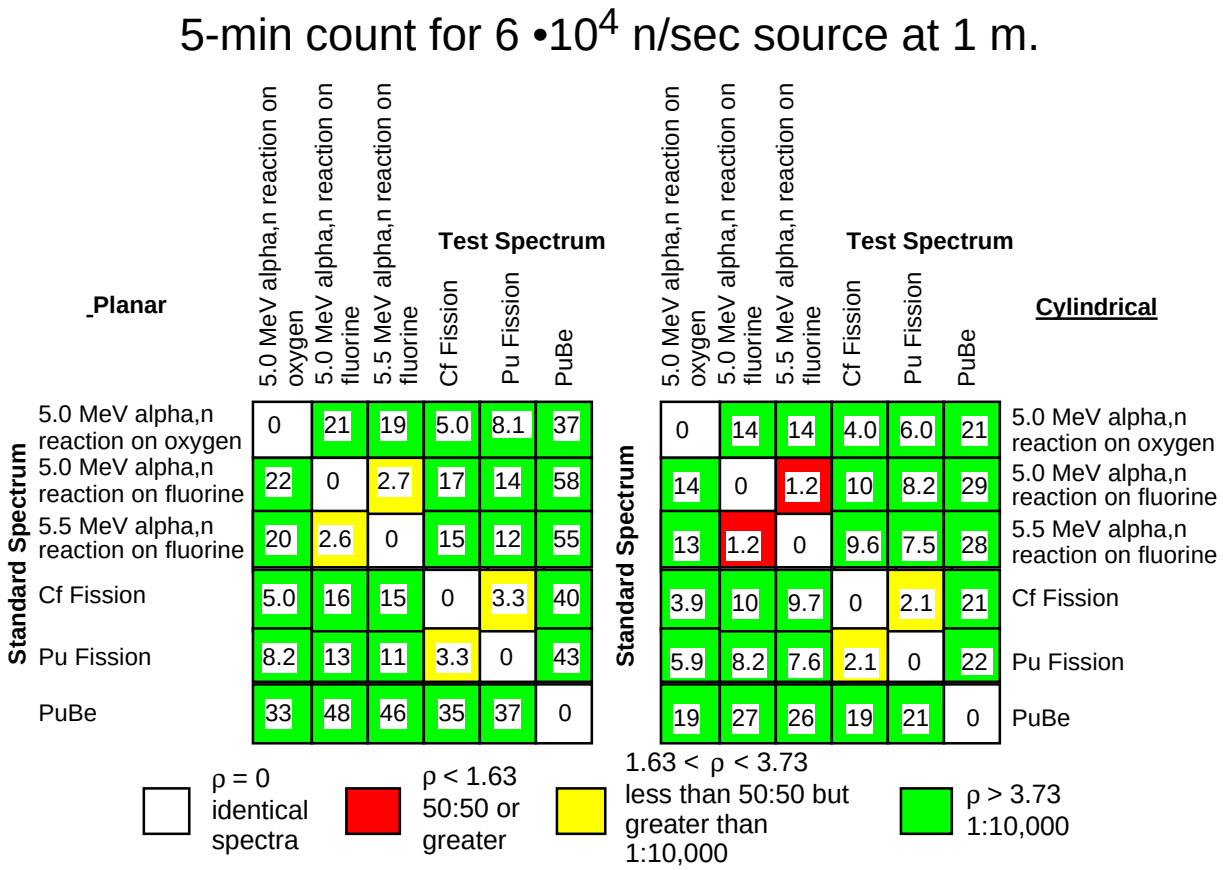

Figure 6.2b. Predicted Weighted Mean-Square Distance Performances of Planar and Cylindrical Spectrometers for the Fixed-Count Scenario. The weighted mean square distance for each situation is shown in the respective box. Values of $\rho = 0$ imply identical spectra; values less than 1.63 mean that the measurement is sufficiently similar to the standard that they have equal probability, or greater, of having been generated by the same spectrum; values of ρ greater than 3.73 mean that there is less than 1 chance in 10,000 that the measurement and standard were generated by the same spectrum.

7.0 Summary

The performance of planar and cylindrical configurations for a fiber-based, moderating spectrometer have been compared relative to each other, and the potential performance of the planar configuration was assessed for various scenarios. All analyses were conducted based on a noise-free assumption; however, statistical variations were explicitly included. Background variations were assumed to be inconsequential. Analyses were conducted with respect to two scenarios and six neutron spectra. For a source with an emission rate approximating that of 1 kg of WG Pu, the planar configuration is found to be superior to the cylindrical.

Both configurations, given sufficient time, were found to be capable of distinguishing between PuBe, 5-MeV Oxygen (α,n), 5-MeV Fluorine (α,n), 5.5-MeV Fluorine (α,n), Cf fission, and Pu fission. With the exception of the 5 and 5.5 MeV Fluorine (α,n), statistically significant (99.99%) discrimination between all spectra can be achieved in about 5 min.

For the fixed-time scenario, with a counting period of 5 min, each of the designs is able to distinguish between all of the neutron spectra, except the two Fluorine (α,n) spectra, such that the chances of statistical noise causing a like to be mistaken for an unlike (or vice versa) to be less than 2%; for most spectra, the chances are many orders of magnitude smaller.

For the fixed-total-number-of-counts scenario, with $3.5 \bullet 10^4$ total counts, which takes about 5 min, the performance is similar with all separations (excepting the two Fluorine spectra) better than 98% confidence, and in most cases better than 99.9999%.

Either scenario is capable of distinguishing the WG Pu-metal fraction in mixes with WG PuO to 20% with better than 98% confidence in about 20 min, when the emission rate is that of approximately 3 kg of metallic WG Pu.

A scenario was examined in which the fixed parameter is the total count in one of the layers. This scenario was found to be advantageous in separating some spectra, particularly the separation of various mixes of WG Pu metal and WG PuO.

From these results, it is clear that the fibers allow the design of a highly intelligent, highly flexible, portable spectrometer system that is capable of distinguishing between similar spectra. For some applications, the simplicity of this design may provide an additional benefit because its mode of operation and capability is simple and readily understood by one skilled in neutron physics. In addition, this analysis demonstrates that a choice of planar configuration is statistically well justified for general application. A cylindrical configuration is slightly more efficient, although its performance is slightly poorer; in some applications, this configuration may, on balance, have a technical advantage that offsets the difficulty in engineering.

The data allow analysis of the information content of the individual fiber layers. This is done in Appendix A. An analysis of the effect of environmental variation on performance is presented in Appendix B. The planar spectrometer configuration has a front and a back, both of which have polyethylene layers that, in operation, may be removed. An analysis of the effect of changing the configuration on performance is presented in Appendix C.

Presently, a planar spectrometer is under construction. It is expected that the performance of the actual detector may be improved, relative to this analysis, by adding information arising from gamma-ray interactions with the fiber.[1]. When the detector has been tested, and information on such properties as noise and the value of gamma-ray interactions obtained, the idealizations of this analysis can be lifted. Among other things, then an inversion protocol can be developed to let the detector perform as a true spectrometer.

[1] If the variables become neutron count and gamma-ray count in each fiber layer, the dimensionality increases from 6 to 12. The probability density for ρ then becomes $P(\rho)= C\ \rho^{11}\exp(-\rho^2)$, where C is a normalization constant. The increased dimensionality increases the peak value of ρ from 1.58 to 2.35 and increases the 1% value of ρ from 2.90 to 3.62. Proportionately, the additional dimensionality is justified only if the additional information gleaned from the added data increase the values of ρ.

8.0 References

Bliss, M., and R. A. Craig. 1995. "A Variety Of Neutron Sensors Based On Scintillating Glass Waveguides," in *Pacific Northwest Fiber Optic Sensor Workshop*, Eric Udd, Editor, Proceedings SPIE Vol. 2574; pp. 152-158.

Bliss, M., R. L. Brodzinski, R. A.Craig, B. D. Geelhood, M. A. Knopf, H. S. Miley, R. W.-Perkins, P. L. Reeder, D. S.Sunberg, R. A. Warner, and Ned A. Wogman. 1995. "Glass-fiber-based neutron detectors for high- and low-flux environments," in *Photoelectronic Detectors, Cameras, and Systems,* C. Bruce Johnson, Ervin, J. Fenyves, Editors, Proc. SPIE 2551,108-117.

Bliss, M., R. A. Craig, and D. S. Sunberg. 1997. "Spectroscopy Without a Spectrometer," in *Proceedings of the Pacific Northwest Workshop on Fiber-Optic Sensors,* Troutdale, Oregon, May 1997.

Good, M. S., N. H. Hansen, P. G. Heasler, H. A. Undem, J. L. Fuller, and J. R. Skorpik. 1993. *Intrinsic Signatures of Polymer Based Fiber Reinforced Composite Structures: An Ultransonic Approach*, PNL-SA-22408, Richland, Washington.

Hezeltine, P. L., M. Bliss, R. A. Craig, and D. S. Barnett. 1998. "Nuclear Fingerprinting With a Scintillating Fiber Detector," *Proceedings of the 1998 Meeting of Institute of Nuclear Materials Management,* Naples, Florida.

Knoll, Glenn F. 1989. *Radiation Detection and Measurement*, Second Edition, Wiley, New York.

Matsunobu, H., T. Oku, S. Iijima, Y Naito, F. Masukawa, and R. Nakasima. 1992. "Data Book for Calculating Neutron Yields from (α, n) Reactions and Spontaneous Fission," *Japan Atomic Energy Research Institute,* JAERI-1324.

Seymour, R. S., B. Richardson, M. Morichi, M. Bliss, R. A. Craig, and D. S. Sunberg 1998. "Scintillating-Glass-Fiber Neutron Sensors, Their Application and Performance for Plutonium Detection and Monitoring," in *proceedings of the International Conference on the Safety of Radiation Sources,* September 1998.

Toyokawa, H., M. Yoshizawa, A. Uritani, C. Mori, N. Takeda, and K. Kudo. 1996. "Performance of a Spherical Neutron Counter for Spectroscopy and Dosimetry," *Nucl. Inst. and Meth.* **A 381**, 481.